energy&fuels
Article
pubs.acs.org/EF

Pairing Integrated Gasification and Enhanced Geothermal Systems (EGS) in Semiarid Environments

Divya Chandra,[†,§,‡] Caleb Conrad,[†,‡] Derek Hall,[†,§] Nicholas Montebello,[†] Andrew Weiner,[†] Sarma Pisupati,[†] Uday Turaga,[§] Ghazal Izadi,[†,‡,§] Arun Ram Mohan,[†,§] and Derek Elsworth*[,†,‡,§]

[†]Energy and Mineral Engineering, [§]EMS Energy Institute and [‡]G3 Center, Pennsylvania State University, University Park, Pennsylvania 16802, United States

[§]ADI Analytics LLC, Houston, Texas, United States

ABSTRACT: We explore the feasibility of combining the circulation of supercritical CO_2 in EGS reservoirs with integrated gasification combined cycle (IGCC) power generation. The symbiotic benefits of this pairing increase net power output over the use of either system in isolation, reduces water use per MWe, and substantially reduces fugitive emissions over conventional thermal power plants. A prototypical plant set in the arid southwestern U.S. (environs of Albuquerque, NM) could sustain anticipated circulation rates of 800−1600 kg/s of CO_2 in a 200 °C reservoir, resulting in a thermal output of ∼150−300 MW-thermal to augment the 550 MW from IGCC. This design would reduce annual emissions by 8,200 tons of NOx, 20,000 tons of SO_2, and 4.35 million tons of CO_2 over conventional thermal plants in an optimal pairing.

1. INTRODUCTION

Critical issues related to the viability of enhanced geothermal systems (EGS) include (i) the high cost of drilling and the routine availability of high geothermal gradients, (ii) the ability to create a low-impedance, high-heat-transfer reservoir that is both hydraulically and thermally long-lived, and (iii) the availability of a low cost heat transfer fluid or the likelihood of minimal fluid losses in the subsurface. In addition to these principal economic constraints the apparent necessity for the system to be environmentally benign, especially with respect to triggered seismicity, appears important. Of these constraints issues of access to the reservoir (item (i)) and the abundant availability of a heat transfer fluid (typically water, item (iii)) are conditioned by the geographic location of the site and its geological setting.

Within the United States, the depth to reach a hot reservoir is minimized if the high heat-flow areas of the western U.S. are used − and thus drilling costs are concomitantly reduced. However, the western U.S. is arid and water is a scarce and valued resource. Correspondingly the substitution of alternate heat transfer fluids, such as CO_2 offers clear advantages if readily available. The most readily harnessed source of CO_2 is from thermal electric generation. However, normal thermal plants suffer two principal drawbacks. They have both high fugitive water losses and require extraordinary efforts to capture a purified stream of CO_2 from the dilute flue gas emission. One alternative to this is to use either oxy-combustion or integrated gasification combined cycle plants that mitigate these two problems − they provide both a concentrated efflux of CO_2 that may be used as the injection fluid for $scCO_2$-EGS and they have reduced water usage over conventional thermal generation systems.

The following explores the use of the symbiotic linkage of high enthalpy EGS circulated by supercritical CO_2 ($scCO_2$-EGS) with concurrent electricity generation by an integrated gasification combined cycle plant (IGCC). A schematic of this pairing is shown in Figure 1. The prototypical setting is within the high heat-flux region of the Rio Grande Rift in New Mexico, U.S. We examine the feasibility of the pairing of these methods and size a plant that optimizes the above surface and subsurface attributes.

2. SUPERCRITICAL-CO_2-EGS ($scCO_2$-EGS)

The subsurface system comprises the usual attributes of an EGS system where water is substituted by supercritical CO_2.[1,2] This design requires knowledge of the geological setting and the ability to develop and sustain a low-impedance but high-heat-flow reservoir and to mitigate triggered seismicity but with the added complication that the heat transfer fluid is $scCO_2$. The principal challenge is that despite the many demonstration projects conducted to date, no single project has utilized any fluid other than water as the circulating medium − it is entirely without precedent.

We explore the principal issues related to a $scCO_2$-EGS plant in the Rio Grande Rift. These relate to the geological setting and thermal and physical conditions of the reservoir, the potential geometry of the reservoir and thermal behavior and the anticipated form of triggered seismicity. We use this information, in particular an understanding of thermal drawdown within the reservoir, to pair the subsurface plant with the above-surface IGCC facilities.

2.1. Reservoir Characteristics. Critical in the development of a viable EGS reservoir is the ability to create a low-impedance high-heat-transfer-area connection between wells in hot rock. Intrinsic to this is that the reservoir rocks must be of sufficiently low permeability to prevent excessive leak-off but allow an engineered hydraulic connection to be formed. These characteristics are controlled by the geophysical characteristics at reservoir depth.

2.1.1. Geology and Structure. The selected prototypical location is the Rio Grande Rift Basin that has higher than average

Received: August 26, 2012
Revised: October 29, 2012
Published: October 29, 2012

   dx.doi.org/10.1021/ef301397n | Energy Fuels 2012, 26, 7378−7389

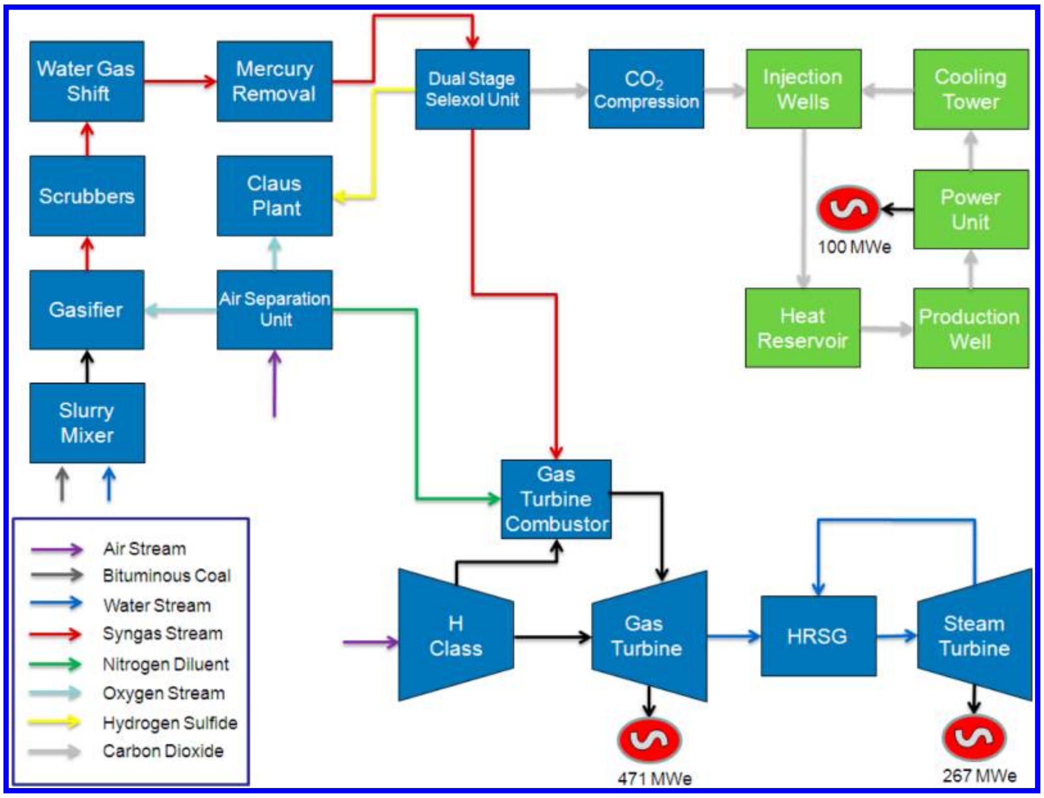

Figure 1. $scCO_2$-circulated EGS combined with IGCC system.

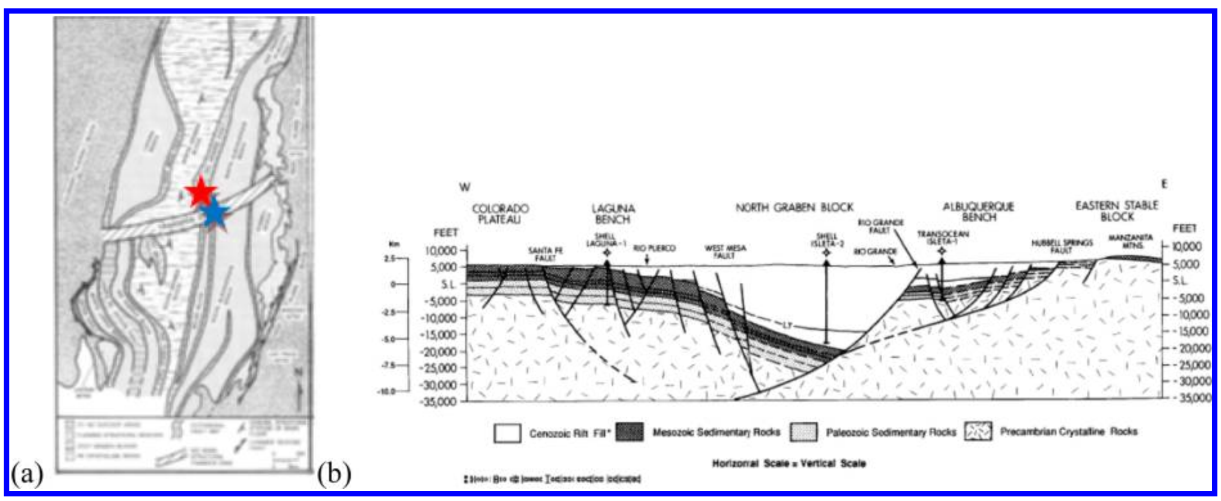

Figure 2. (a) Generalized structural framework of the Albuquerque basin depicting the structural configuration of the Pretertiary "basement"[4] [red star denotes approximate location of Albuquerque, NM and blue star denotes approximate study area]. (b) Seismic section illustrating the structural configuration of the southern portion of the North Albuquerque basin.[4]

heat flow. The Rio Grande Rift Basin is a prominent geologic feature that stretches from South Central Colorado into Mexico. The formation of the Rift Basin began approximately 30 Maago and has continued until the present.[3] The structure of the Albuquerque Basin is dominated by the rifting events in the greater geographic region. Specifically, the Albuquerque Basin is divided into two sub-basins termed the north basin and the south basin (Figure 2). The two basins are the product of two different down-dropped grabens. The partition between the two basins is a transfer zone.[4] The northern basin is controlled by a west-dipping listric normal fault.[4] The southern basin is controlled by the east dipping Sante-Fe, Cat Mesa, and Jeter Faults.[4] Any reservoir must be located in the blocks bounded between these faults where pristine rock will limit fugitive fluxes.

The formations within the Albuquerque Basin can be divided into Precambrian crystalline basement rocks, prerifting Paleozoic and Mesozoic Sedimentary rocks, and rifting Cenozoic basin fill and volcanics. The target formation for the EGS system is the Precambrian basement rocks which are granites, gneiss, schists, greenstones, and quartzites. These rocks typically form the rim around the basin and occur at depth within the basin.[5]Within the basin either Mississippian aged or Pennsylvanian aged limestone and marine shale rest above these basement rocks but include an intervening delay (unconformity) between periods of deposition.

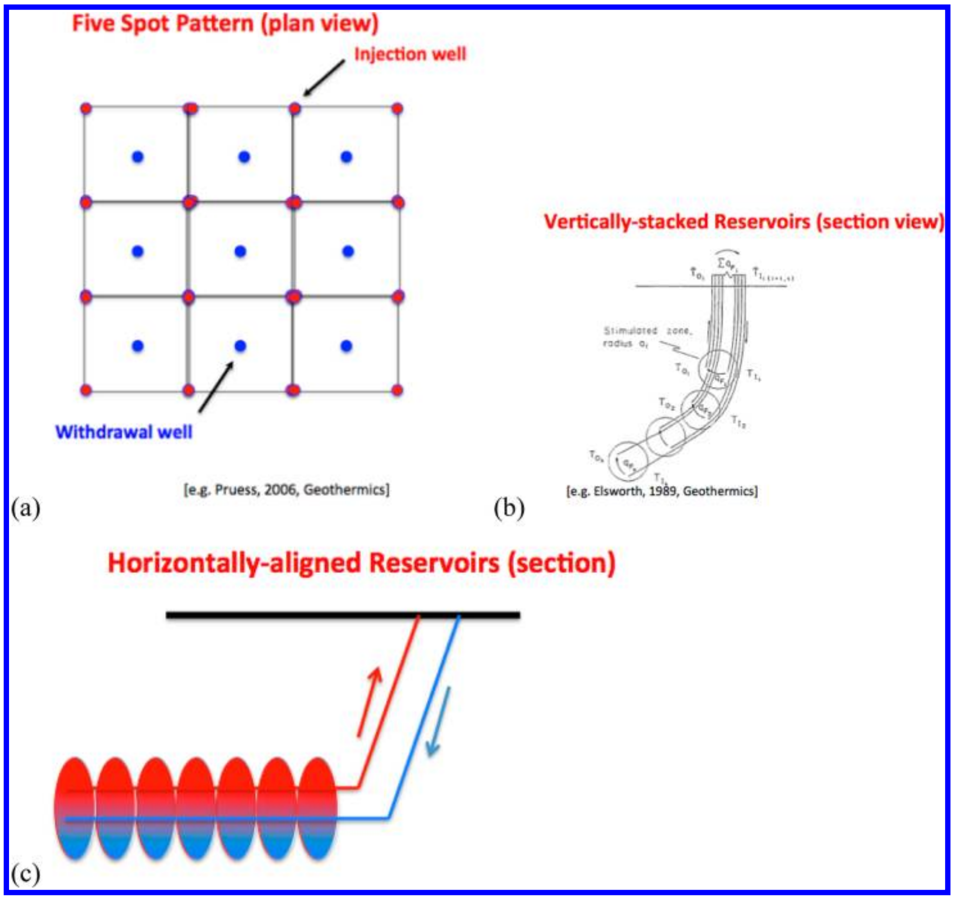

Figure 3. (a) Five spot and (b) vertically and (c) horizontally stacked reservoir configurations.

The proposed location of the site is within the Northern Albuquerque Bench near the Transocean Isleta-1 exploratory hydrocarbon well (Figures 2a (plan view) and 2b (cross section view)). The stratigraphy in the area of the Northern Albuquerque Bench (Figure 2b) exhibits a more gentle westward dip than the beds found closer to the center of the basin. This rotation is a product of the tectonic history of the rift system.[4] Furthermore it can be observed that there is a deep detachment surface which dominates the seismic section with smaller graben existing within the larger slip feature.

This area is very close to the Rio Grande Fault and the Hubbell Springs Fault. Seismic reflection profiles and petroleum wells that terminate at the top of the basement rocks are available close to the proposed site location.[4] Furthermore additional work completed by ref 6 captures the larger faults and the smaller faults with high resolution aeromagnetic surveys that have surface expressions. There is a strong likelihood that there are more faults in the subsurface that possess weak to no surface expression that could significantly affect subsurface flow.

The combination of low permeability basement at shallow and accessible depth and the wide spacing of known faults at proposed reservoir depth (5 km) provide a voluminous reservoir within fault blocks that is widely separated from potable groundwater resources (above 500 m) – mitigating risk to these resources.

2.1.2. Geothermal Resource. The New Mexico Rio Grande Rift Basin has been the subject of much geothermal exploration with the data organized into many different formats[7−10]with many other reports on spring temperatures, spring chemistry, geothermal municipal wells, and geothermal oil and gas wells. The site selected for this project is near Transocean Isleta-1 well and is selected due to satisfactory depth to Precambrian basement rocks (~3.2 km), a high geothermal gradient (39 °C/km) and resulting high bottom-hole temperature (131 °C), and large thickness of the Precambrian basement rock that could be penetrated to create a reservoir (~1.8 km).[11] If the geothermal gradient that was determined for the Transocean Isleta-1 well holds true, then a bottom-hole temperature of ~200 °C is expected at a depth of 5 km.

2.1.3. Geophysical Properties of the Reservoir. The characteristics of the reservoir rocks are defined based on regional lithotypes. Anticipated regional *in situ* permeabilities are of the order of a millidarcy (e.g., Coso, Rosemanowes, Soultz, and others) with matrix rocks of the order of a microdarcy or lower. Fracture spacings are undefined but are anticipated in the 10−100 m range and would provide seed structures for generating connected fracture networks at depth. For the remainder of this work we use magnitudes of geophysical properties in the range of those recovered from active EGS demonstration projects located in crystalline basement – similar to the crystalline basement here.

2.2. Thermal Evolution of the Reservoir. A variety of issues relate specifically to interfacing $scCO_2$-EGS with IGCC. These include all the reservoir interaction behaviors important in ensuring the viability of EGS: *viz.* reservoir stimulation and development concurrent with developing heat-transfer area within the reservoir. For $scCO_2$-EGS these include the important and poorly defined role of fluid-rock interactions and their impact on permeability, heat-transfer area, and strength characteristics of the reservoir. The latter is ultimately related to production-induced seismicity and the related development of permeability by hydroshears. Although these issues are crucial and relate fundamentally to the viability of $scCO_2$-EGS they are beyond the scope of this work. Here we limit ourselves to the highest-level linkages between $scCO_2$-EGS and IGCC − these relate to anticipated thermal output from such a system and the mechanisms of interfacing the output stream with IGCC *via* surface plant. We discuss only the issue of thermal output in the following in particular related to the anticipated thermal drawdown within the reservoir. This analysis relies on the selection of (i) an appropriate reservoir configuration and (ii) appropriate mechanistic models for thermal drawdown.

2.2.1. Reservoir Configurations. A variety of potential configurations exist for reservoir development. For the demonstration-level projects currently observed, these configurations have typically been a doublet (single injector and producer) or flanked doublet (single injector flanked by dual producers split from a single surface hole). This configuration is peculiar to demonstration projects as it provides the most effective and lowest-cost access to a deep reservoir. However, for large-scale development, this configuration is likely to be supplanted by other well configurations [Figure 3]. Typical within the petroleum field is the repeating "five-spot" pattern.[2] This regular grid is common in shallow regular reservoirs but is disadvantaged where the reservoir is deep as it requires multiple deep wells to access the reservoir zone. Alternative configurations are to examine vertically stacked reservoirs[12] or horizontally aligned reservoirs, now feasible with advances in horizontal drilling technology. In particular horizontal drilling maximizes the ability to source multiple holes from the bottom of a single inclined hole and to thereby maximize the volume of the reservoir accessed relative to the drilling cost.[13]It is not clear whether drilling technology in hard rock is sufficiently advanced to allow the latter, but this may be a necessary development to allow the viability of such projects. In all of these instances, the reservoir is typically stimulated from a single injector well, and secondary withdrawal wells then drilled to intersect the fringes of the stimulated reservoir volume.

There is poor control on the evolving size and shape of the engineered reservoir, these features are controlled by the specifics of the stress field and the relic structure at depth. Thus, in this work we examine the drawdown of the reservoir related to injector-withdrawal doublets that are insensitive to the specifics of the well layout and more sensitive to fracture spacing − thus the solutions herein are valid independent of the drilling layout. The results are correct for the principal controlling parameters. These are fracture spacing, defining heat transfer rate to the fluid, and mass flow rate through the reservoir, defining and the rate as which this acquired heat may be removed from the reservoir. The principal assumption is that the fluid sweep is uniform and does not short-circuit from inlet to outlet (a current grand challenge in EGS systems). The reservoir geometry and other parameters used for simulation are summarized in Table 1. The data used for simulation is collected from the available literature.

2.2.2. Thermal Drawdown Analysis. As discussed earlier, largely independent of the specific well configuration, thermal drawdown within the reservoir may be evaluated with knowledge of the thermophysical properties of the reservoir rocks and circulated fluid and the geometry of the transport connections within the reservoir. For first order analysis, spherical reservoir and parallel flow models are reasonable candidates to represent behavior [Figure 4]. The spherical reservoir model (SRM)

Table 1. Thermophysical Material Parameters Appropriate for $scCO_2$-EGS Reservoir Modeling

	rock	water	$scCO_2$	units
thermal conductivity	2.1	0.6	0.015	W/m·K
density	2600	1000	231	kg/m^3
specific heat capacity	1000	4181	1364	J/kg·K
thermal diffusivity	81	14	4.8	$\times 10^{-8}$ m^2/s

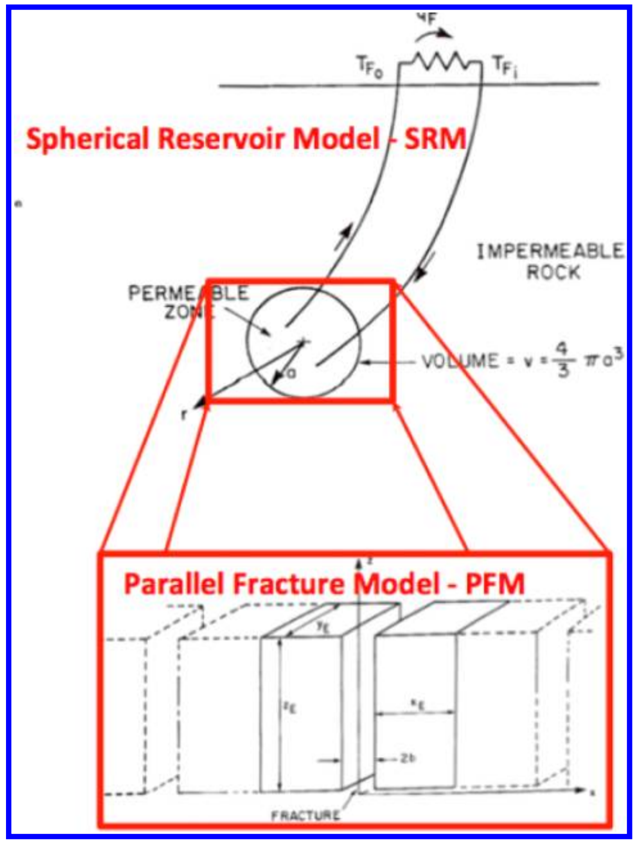

Figure 4. Congruence of spherical reservoir (SRM) and parallel fracture (PFM) models to represent deep EGS reservoirs.

assumes that both the reservoir and circulated fluids are at thermal equilibrium with temperatures augmented by heat supply from the far-field by conduction.[12,14]This model gives adequate estimates for heat supply where fracture spacing within the reservoir is small but overestimates thermal output where spacing is large. Where fracture spacing is large the parallel fracture model (PFM) provides better estimates of thermal output and of thermal drawdown although the boundary of the reservoir is assumed thermally isolated and no supplemental heat supply is possible.[15,16] In practice this latter constraint is of second-order importance and thermal drawdown may be evaluated from knowledge of the previous thermophysical properties supplemented by reservoir volume, fracture spacing, and fluid throughput.[17]

The appropriate thermophysical properties for the reservoir and fluids are given in Table 1. The nondimensional thermal drawdown (T_D) scales with three other nondimensional parameters of flow rate (Q_D), time (t_D), and fracture spacing (x_D).[17] These are

dx.doi.org/10.1021/ef301397n | *Energy Fuels* 2012, 26, 7378−7389

$$T_D = \frac{T_{Fi} - T_{Fo}}{T_{Fi} - T_R}; \qquad Q_D = \frac{q_F \rho_F c_F}{\lambda_R a}; \qquad t_D = \frac{\lambda_R t}{\rho_R c_R a^2}; \qquad x_D = \frac{x_E}{a} \tag{2.1}$$

where subscripts are for fluid (F) and rock (R), reservoir inlet (i) and outlet (o), and other variables are for flow rate (q), density (ρ), specific heat capacity (c), thermal conductivity (λ), reservoir radius (a), fracture spacing (x_E), and time (t).

Where the thermophysical parameters of Table 1 are used, the thermal drawdown of candidate $scCO_2$-EGS reservoirs may be evaluated. We assume a doublet well spacing of 500 m as a reasonable candidate separation, fracture spacing in the range 10−100 m, and fluid circulation rates of 100 and 1000 kg/s of $scCO_2$ within the reservoir. These mass circulation rates are not necessarily for individual doublet systems which for water injection have been limited to less than ∼100 kg/s. However, these required flow rates are dictated by the output of the IGCC, as will be discussed later. The relative flow rates may be evaluated from the ratio $q_f^{CO_2}/q_f^{H_2O}$. Thus the relative mass rate relates to the ratios of the mobilities of the fluids − the ratios of density to viscosity as

$$\frac{q_f^{CO_2}}{q_f^{H_2O}} = \frac{\rho^{CO_2}}{\mu^{CO_2}} / \frac{\rho^{H_2O}}{\mu^{H_2O}}$$

Thus for typical magnitudes of these ratios for reservoir conditions at 5 km (200C and 50 MPa) the flow is enhanced by a factor of ∼1.5 for the circulation of CO_2 relative to that of water. The resulting rates of thermal drawdown for these circulation rates are shown in Figure 5 for the SRM and PFM models.

2.2.3. Thermal Drawdown in Prototypical Reservoir. Thermal drawdown within the PFM occurs most rapidly for circulation at 1000 kg/s. Where the fractures are widely spaced (100 m) thermal supply to the circulating fluid is conduction-limited and the reservoir cools rapidly - the reservoir lifetime is of the order of months. Reservoir lifetime is extended for more narrowly spaced fractures, and the reservoir approaches a condition of being flow-rate limited as evident in the steep decline curve of Figure 5. In this configuration, the thermal drawdown is similar to that of the SRM as in each instance the fluid and average rock temperatures are in equilibrium. However, at this rate of circulation the thermal drawdown is still too severe to be commercially viable limiting the reservoir lifetime to only a few years. However the reservoir lifetime is extended where the circulation rate is reduced. Where the circulation rate is reduced to 100 kg/s the reservoir approaches a state of thermal equilibrium even for widely spaced fractures (100 m) and reservoir lifetimes (50% drawdown) are congruent for SRM and PFM as of the order of 20−50y. Thus, limiting rates of circulation (100 kg/s), reservoir volumes (one-eighth of a cubic kilometer), and fracture spacing (<100 m) are defined as feasible for reservoir lifetimes of the order of 30 years.

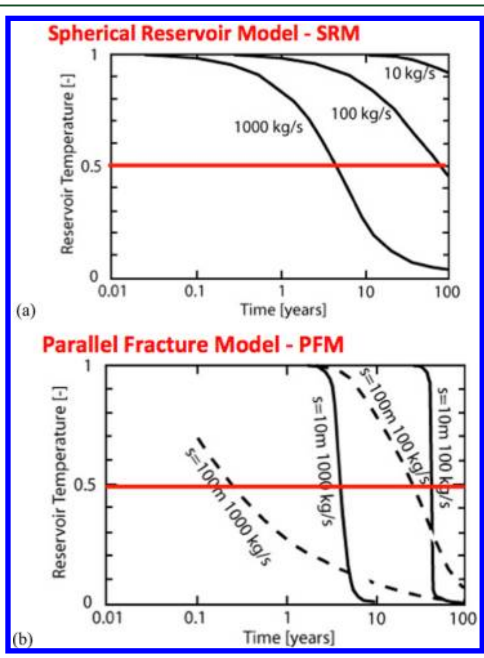

Figure 5. Thermal drawdown (T_D) with time for $scCO_2$ circulation at rates of 100 and 1000 kg/s for fracture spacing within the reservoir of 10 m and 100 m. Reservoir is 0.125 km^3, and results are for (a) spherical and (b) parallel fracture models.

These estimates are consistent with observations scaled from other demonstration projects, most notably the drawdown rates observed at Fenton Hill (USA) and at Rosemanowes (UK) as illustrated in Figure 6.

2.3. Triggered Seismicity. Mitigating the effects of triggered seismicity is important in the development of the reservoir. The energy release (E_p) from a single rupture event on a pre-existing fracture scales with the stress drop ($\Delta\tau$), radius of the fracture (a), and shear modulus of the surrounding material (G) as

$$E_p = \frac{2\Delta\tau^2 a^3}{3G} \tag{2.2}$$

defining the important unknowns that control the magnitude of any seismic event. Stress drops are typically of the order 1−10 MPa, and shear modulus is of the order of 10 GPa, leaving the fracture size as the main discriminating feature. The energy release may be converted into a moment magnitude as[18] $\log M_0 = 1.5M_s + 9.1$ where M_0 is seismic moment and M_S is moment magnitude. In this model M_0 is seismic energy which is derived from the elastic energy released (E_p) by shear on pre-existing fractures. We initially consider the specific times at which seismic activity occurs as a function potential and total energy. The distribution of moment magnitudes with time, due to combined thermal, mechanical, and chemical effects[19] for a reservoir seeded with 200 m fractures is illustrated in Figure 7.[20] This outcome indicates that the potential energy within the reservoir containing fracture networks is released with time and penetrates far into the reservoir from injection. The principal implication of this is that the strain energy of the reservoir becomes progressively depleted with time as it is released seismically. This depleted energy is not replaced. This gives reasonable magnitudes for anticipated events but for pre-existing natural fractures of the order of 200 m in length. Larger fractures result in larger magnitude events with the energy release scaling with the cube of fracture length.

2.4. Geothermal Energy Conversion System. The geothermal resource at the selected site is at the cusp of either a binary or a double flash energy conversion system if the working fluid was only water. The expected pressures and temperatures within the reservoir are firmly within the liquid phase envelope of water and within the supercritical region of carbon dioxide. In addition to the phase behavior of the water and carbon dioxide mixture, its corrosive nature must be accounted for within any conversion system due to lifespan concerns. To overcome the phase behavior differences of the two

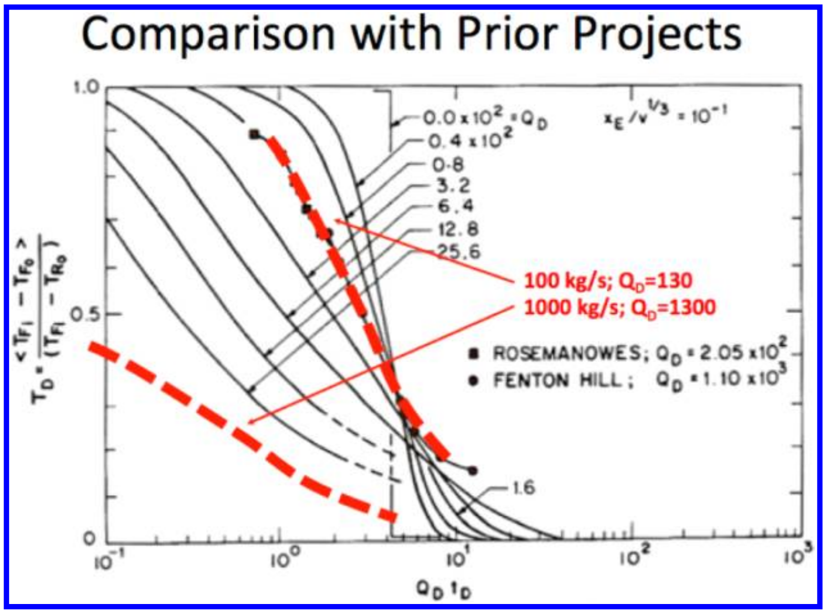

Figure 6. Scaled rates of drawdown for recovery at 1000 and 100 kg/s for the prototypical reservoirs considered here and for prior demonstration projects at Fenton Hill (USA) and at Rosemanowes (UK).[17]

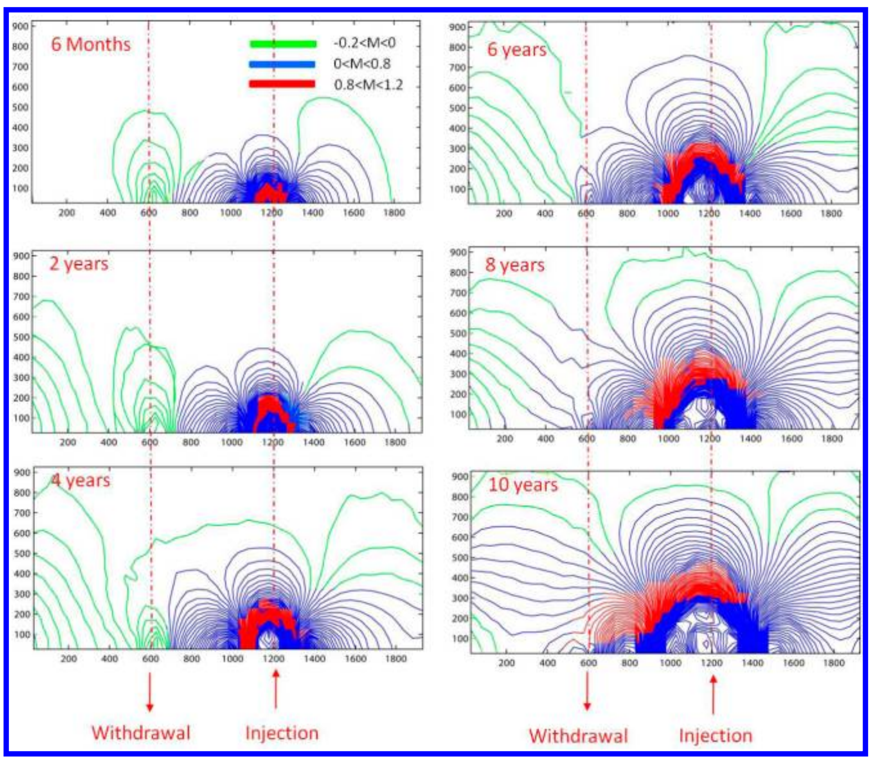

Figure 7. The evolution of moment magnitude in an EGS reservoir for a pre-existing 200 m-long fracture over 10 years of simulation. Solid lines illustrate the failure in each location of reservoir. The green region represents the smallest event magnitude and the red the largest potential energy that is released in different locations due to thermal, mechanical, and chemical effects.

fluids and to maximize electricity generation, the produced fluids will go through a separation process that creates a $scCO_2$ stream and a water stream. A schematic is shown in Figure 8. The Geothermal Energy Conversion System is formed of three main components: (i) gravity separator, (ii) $scCO_2$ turbine, and (iii) flash system.

2.4.1. Gravity Separator. The gravity separator that is required for this site must be flexible in order to match the evolving characteristics of the produced fluids. Broadly the produced fluids can be divided into three distinct time periods. These periods are (1) Early time, when only water is produced; (2) Intermediate time, when a water dominated mixture of water and $scCO_2$will be produced; and (3) Later time, when a carbon dioxide dominated mixture of water and $scCO_2$ will be produced. A vapor−liquid phase gravity separator will be used to create the water stream and the $scCO_2$ stream for electricity production. This is a necessity to maximize electricity production. For water it

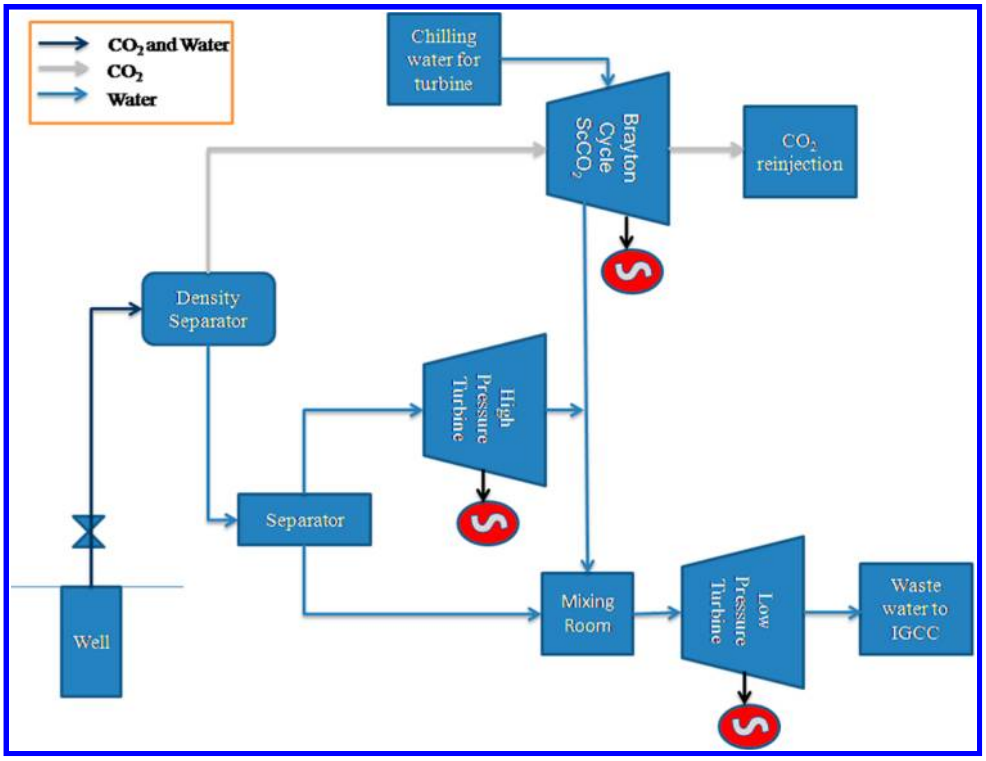

Figure 8. Block diagram of the Geothermal Energy Conversion System.

is desirable to shift the phase to near standard conditions but not so for the $scCO_2$ stream.

The gravity separator is a vertical vessel and separation results from settling and sedimentation driven by gravity. Liquid droplets will settle out of the gas phase if the gravitational force acting on the droplet is greater than the drag force of the gas flowing around the droplet or particle.[21] Gravitational forces influence separation; the liquid/gas separation will be more efficient with a low gas velocity and the large vessel size.[21]The separator dimensions are sized to match the 1000 kg/s flow rate of fluids plus a safety factor to account for potential increases of flow rates over the lifetime of the reservoir.

2.4.2. $scCO_2$Turbine. The proposed power plant accommodates the dual water and $scCO_2$ streams inherent in the process. After separation the produced water will flow through a double flash geothermal system if economical quantities of water are produced. The $scCO_2$ stream will flow from the gravity separator into an unrecuperated Brayton cycle turbine. The turbine has high efficiency, and it is designed to operate with $scCO_2$ as the working fluid. Recent work at Sandia National Laboratory suggests that this turbine will be capable of performing within the prevailing conditions of the system at the site with substantial benefits such as the ability to remove the compressor and combustion sources from the system because the $scCO_2$ exits the reservoir preheated and at elevated pressures and after water separation arrives at the Brayton turbine ready for power generation.[22] The additional energy is generated from the heat rejection of the $scCO_2$ gas. The water stream is passed through the gas chiller to extract the heat from the $scCO_2$fluid. Compared to other gas turbines the $scCO_2$ turbine could increase the electrical power produced per unit of fuel by 40% or more.[22]

With a flow rate of 1000 kg/s $scCO_2$ and pressure ratios of 1.8, the turbine will generate 15 MWe and 100 MWe will be generated from the heat rejection of the $scCO_2$. The EGS plant performance is defined in Table 2. A Brayton cycle engine has not been applied to $scCO_2$ associated with geothermal resources as of yet, and a significant design concern for the turbine is the mass flow rate of corrosive $scCO_2$ over the lifetime of the reservoir. The size of the turbine is based on the mass flow rate of $scCO_2$. During initial times it is expected that the flow rate of $scCO_2$ will be less than flow rates at later times. This may require a low mass flow turbine as well as a high mass flow turbine to efficiently generate power.

Table 2. Plant Performance of EGS Plant[22]

parameter	value
$scCO_2$ turbine, kWe	14,285
energy from heat rejection, kWe	100,000
total auxiliaries, kWe	9,142
total power, kWe	114,285
net power, kWe	105,143

For this plant it is necessary to reinject carbon dioxide into the reservoir at supercritical conditions. The $scCO_2$ coming out of the turbine will not be required to recompress prior to reinjection, as the pressure loss will be reduced due to the low pressure ratio of the turbine and CO_2which will be in the supercritical form. Allowing the $scCO_2$ to remain in the supercritical state throughout the energy conversion process will minimize parasitic loads associated with phase change of the subcritical carbon dioxide to supercritical conditions prior to reinjection. This is the most energy-efficient procedure to allow the $scCO_2$ to remain at supercritical conditions while maximizing energy production.

2.4.3. Flash System. The double flash conversion system uses two constant enthalpy pressure decreases to create steam both at high pressure and a lower pressure. Typically the outflow at high pressure is fed into the lower pressure steam flow, allowing additional recovery of electrical generation capacity. This additional efficiency will be required to maximize energy

dx.doi.org/10.1021/ef301397n | Energy Fuels 2012, 26, 7378−7389

conversion during the initial field development until $scCO_2$ begins to be produced. The necessity of a double flash system will be directly related to the volumes of water that are produced at early and intermediate times during reservoir development. The amount of water that will be produced is highly dependent upon the initial water saturation of the reservoir - the cutoff saturation will be approximately 30%. If the saturation is above this value, then water will be produced, but if it is below this value, then no water will be produced. If no or minimal water is produced, then the double flash system will not be required. If significant water is produced, then a double flash system may be worthwhile.

2.5. Thermal Output. With feasible limits placed on circulation rates to ensure a long-lived reservoir, the thermal output may be straightforwardly evaluated from the product of mass flow rate, injection-to-withdrawal temperature differential, and specific heat of the working fluid. Thus, the thermal output (W_{th}) is defined as

$$W_{th} = q_F \rho_F (T_{Fi} - T_{Fo}) c_F \tag{2.3}$$

where all terms are as defined previously. Since the IGCC plant is merely supplying the makeup CO_2 to replace leak-off losses, then the circulation rate of the $scCO_2$-EGS system is in direct proportion to the makeup volume rate. For presumed losses of 5%−10% the ultimate reservoir circulation volumes are in the proportion of 20−10 times the IGCC output rates, respectively. Thus IGCC-$scCO_2$ production rates of the order of 80 kg/s (Table 3) translate to $scCO_2$-EGS circulation rates of the order of 800 kg/s (10% loss) to 1600 kg/s (5%). For a presumed reservoir temperature of 200 °C and a reinjection temperature of 40 °C the thermal drop across the system is 160 °C. This results in an augmented upper bound (geo) thermal output of ∼300 MW_{th} (5% loss) to supplement the 550 MW_e from the IGCC.

Table 3. Plant Performance of Precombustion IGCC Plant[25]

parameter	value
syngas HHV at gasifier outlet (KJ/Nm^3)	8,644
sulfur removal (%)	99.7
mercury removal (%)	95
carbon conversion (%)	98
overall CO_2 capture (%)	90.8
gas turbine power kWe	471,000
steam turbine power kWe	267,000
total power, kWe	738,000
total auxiliaries, kWe	190,750
net power, kWe	547,250

3. INTEGRATED GASIFICATION COMBINED CYCLE (IGCC)

For the next generation of coal-based power plants, integrated gasification combined cycle (IGCC) provides a convenient form to interface with $scCO_2$-EGS. This is because the output stream is near pure CO_2, requiring no separation from nitrogen within the flue, and the other combustion products are water from burning the hydrogen produced as synthesis gas from a water shift reaction following the gasification of the coal.

A schematic of the process is shown in Figure 9. Coal water slurry is fed into the gasifier where it is converted into synthesis gas. The raw synthesis gas is processed by various gas cleaning units and compounds including CO_2, H_2S, and mercury are separated from the hydrogen gas stream. The purified hydrogen gas obtained from the gas cleaning units is then used for power generation.

The principal stages involve (i) producing pure O_2 and N_2 streams from separated input air (Air Separation Unit); (ii) the oxygen is then passed into the gasifier and combusted to produce synthesis gas with high CO content (Gasifier); (iii) then the CO is passed through a water gas shift reaction to yield pure H_2 and CO_2 (Water Gas Shift); and (iv) the CO_2 is used for EGS and the N_2 from the Air Separator (i) is used in cocombustion with H_2 to keep the turbine from overheating. Thus inputs of coal, water, and air result in outputs of concentrated CO_2 and water alone, the latter from the combustion of H_2 and air. The principal features of the IGCC that are an advantage to sCO_2-EGS are the development of a pure CO_2 stream that is used as the working fluid and without the necessity of separation from a dilute exhaust. We describe the critical components of the IGCC in the following.

3.1. Air Separation Unit. The air separation unit (ASU) plays an important role in generating clean energy from coal in an IGCC plant. The primary purpose of the ASU is to separate oxygen and nitrogen from air.[23] The separated oxygen is sent to the gasifier for the production of syngas, and separated nitrogen is sent to the turbine where it is used as a dilutent for gas turbines in order to improve efficiency. NOx emissions can be reduced as injected nitrogen inside the turbine helps controls the adiabatic flame temperature of the combustion products.

Of the available methods, cryogenic reduction is preferred to separate the oxygen and nitrogen as it can be readily integrated with the other plant processes. In cryogenic separation the air is first compressed and is pretreated before cooling in order to remove contaminants including water, CO_2, and hydrocarbons. The air is then cooled to cryogenic temperatures and distilled into oxygen and nitrogen. The air separation units will provide 4400 tons/day of oxygen to the gasifier and Claus plant.

3.2. Gasifier. Coal gasification is the most versatile method to obtain energy from the coal. Entrained flow gasifiers are extensively used for IGCC plants because of their fuel flexibility. In entrained-flow gasifiers, coal slurries and the oxidant are fed into the top of the gasifier and result in a fuel rich gasification process which produces a gaseous mixture known as syngas. This gasifier type operates at very high temperatures and in turn melts ash into inert slag. Typical residence time in the gasifier is on the order of a few seconds, and carbon conversion efficiencies are very high because fine coal is fed at high operating temperature which allows the gasification reaction to occur at a very high rate. The tar, oil, phenols, and other liquids produced from devolatization of coal inside the gasifier are decomposed into H_2, CO, and small amounts of light hydrocarbon gases.

For a power plant in the environs of Albuquerque NM, bituminous powdered coal from the San Juan Basin would be gasified in a pure-oxygen environment to produce CO and H_2. Gasification significantly reduces water use over traditional air-combustion thermal methods. For a nominal power output of 550 MWe we require two entrained flow reactors consuming 7000 t/day of coal water slurry and 3500 t/day of oxygen. The gasifier efficiency is estimated using Illinois number 6 with 63% solids content in the coal water slurry. Both reactors operating with an average cold gas efficiency of 70−75% could supply synthesis gas capable of 1000 MWe.

3.3. Gas Cleaning Unit. The synthesis gas formed inside the gasifier consists of different compounds. The raw synthesis gas is passed from various different processes for purification. These processes are described below.

dx.doi.org/10.1021/ef301397n | Energy Fuels 2012, 26, 7378−7389

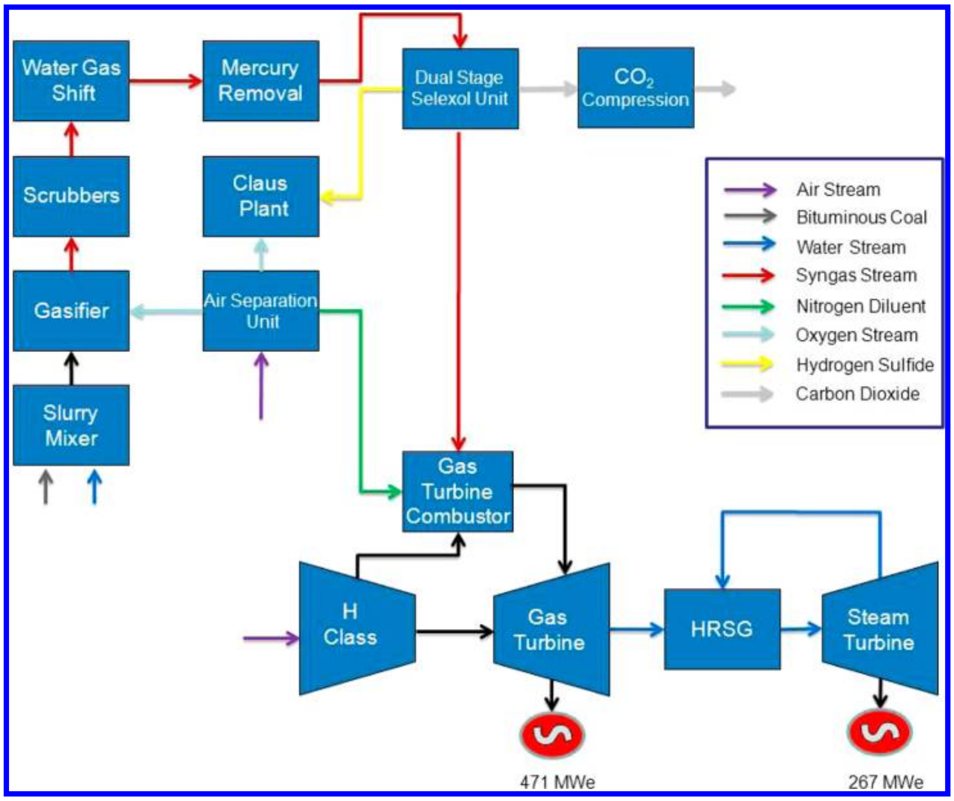

Figure 9. Block diagram of precombustion carbon capture IGCC plant.

3.3.1. Water Gas Shift. The water gas shift (WGS) reaction is between carbon monoxide (CO) and water (H_2O) and is reversible and exothermic. The synthesis gas from the gasifier is primarily composed of CO and H_2 and undergoes the WGS to form a product stream containing mostly H_2 and CO_2.[24]

$$CO + H_2O \leftrightarrow CO_2 + H_2 \tag{3.1}$$

The hydrogen is separated from the product stream and is fed to a turbine for combustion and electricity production.

3.3.2. Mercury Removal. The mercury removal plant operates at a temperature of 35 °C thus the shifted syngas must be cooled down before passing through a fixed bed reactor that contains sulfur-impregnated activated carbon.[25] The excess heat is extracted and transferred to the HRSG in the form of high and medium pressure steam. At high pressures of 6.2 MPa, the activated carbon removes 95% of the mercury in the raw shifted syngas stream. The bed life is estimated to be between 18 and 24 months but is dependent on the actual amount of mercury contained in the coal. Generally over the carbon bed life, the weight percent increase from mercury removal will be 0.6−1.1 wt %; however, the activated carbon could absorb up to 20 wt % maximum but with decreasing rate with time.[25]

3.3.3. Acid Gas Removal. Acid gas removal (AGR) serves to removes acidic gases such as H_2S and CO_2 from the raw syngas stream as aided by physical solvent Selexol.[26]Selexol is polyalkylene glycol dimethyl ether (PGDE).[27] Prior to AGR, the raw syngas stream is cooled down to approximately 25 °C and passed through two consecutive physical absorption columns.[27] The physical absorption of acid gases into Selexol is favored at lower temperatures (25°) and high pressures (5.1 MPa).[28] The reclamation process of procuring the H_2S and CO_2 requires a series of flash drums where the pressure is "flashed" or decreased rapidly thus decreasing the solubility of the physical solution in which the acid gases are captured.[25]The dual stage Selexol process will remove 99.7% of the H_2S from the syngas stream which is then sent to the Claus Plant for further processing.[25]More than 90.3% of the CO_2 is stripped and removed from the acid gas stream.

3.3.3. Claus Plant. The Claus process converts H_2S to elemental sulfur. The following reactions occur in the conversion of H_2S:

$$H_2S + 1.5O_2 \leftrightarrow H_2 + SO_2 \tag{3.2}$$

$$2H_2S + SO_2 \leftrightarrow 2H_2O + 3S \tag{3.3}$$

The Claus process works in many stages including a catalytic stage which consists of gas preheat of a catalytic reactor and a sulfur condenser.[25] Oxygen is required from the Air Separation Unit (ASU) for the first part of the H_2S combustion inside the furnace.[25] Temperatures typically range from 1100 to 1400 °C in the furnace, but higher conversions are achieved at higher temperatures.[28] Assuming the H_2S input stream is at least 20−50% H_2S, a sulfur recovery of 94 to 96% will be achieved.[28]Replacing 15 billion kWh of conventional coal power[29] with zero-emission power generation would save 78,000 tons of sulfur dioxide emissions each year. Using these values, the cumulative power generation from the combined EGS-IGCC plant operating with a capacity factor of 86% provides a yearly savings of 20,000 tons of SO_2 over conventional coal power emissions.

3.4. Power Generation. In an Integrated Gasification Combined Cycle (IGCC) system the "combined cycle" refers to twin turbine cycles: that of a Brayton cycle gas turbine and a Rankine cycle steam turbine. In an IGCC system hydrogen is produced from the gasification of coal, cleaned through various processes, and is then sent to a gas turbine for combustion. The combustion of the hydrogen with oxygen will yield water in the form of steam. The gas turbine effluent steam, at a pressure of 17

MPa and 565 °C, is then fed into the first of a series of three high pressure steam turbines (HPSTs).[30] The effluent from the HPST is then fed into the heat recovery steam generator (HRSG) unit. This HRSG unit has three levels of steam admission, one for each of the three steam turbines: high pressure, intermediate pressure, and low pressure. The relative HRSG pressures and temperatures of these turbine admissions are 2−3 MPa, 538−566 °C; 2−3 MPa, 11 °C; and 0.25 MPa, 11 °C.[30]The anticipated performance of the plant is defined in Table 3. A 550 MW_e plant generates an effluent stream of CO_2 at approximately 80 kg/s. This is used as the makeup fluid for the $scCO_2$-EGS system defined earlier. Combining the net power output of the IGCC with the net power output from the EGS, the final estimate on the combined net power output for the IGCC-EGS system is 650 MWe.

4. BENEFITS OF $SCCO_2$ CIRCULATED EGS-IGCC

Two primary advantages to the combined EGS-IGCC system are a substantial reduction in fugitive emissions to the atmosphere and efficient use of fresh water when compared to the performance of a new pulverized coal plant. Augmenting IGCC technologies with $scCO_2$ EGS provides an opportunity to partially sequester and store the CO_2 produced by the IGCC plant with the added benefit of significantly reducing the water consumption from an EGS system. Ultimately, this unique combination enables a proposed power plant to produce a higher power output per unit mass of water consumed than either IGCC or conventional water-circulated EGS could supply by themselves while sequestering CO_2.

4.1. Water Savings. In an IGCC power plant, the Rankine cycle is relegated to a secondary role in power generation, and the more water conservative Brayton cycle becomes the primary power converter. In conventional coal power plants, 73 to 99% of water consumption comes from inefficiencies in the cooling tower condensers.[25] This shift from a reliance on the Rankine cycle to a Brayton cycle allows for a significant reduction in the amount of water consumed in the large cooling towers. As a result, an IGCC system without carbon capture and sequestration uses approximately 950 kg of water per MWh, whereas a new supercritical coal plant would consume 1600 kg of water per MWh.[31]

For water-circulated EGS, one of the largest sources of water consumption is the fluid losses within the geothermal reservoir. By replacing the mass flow rate with CO_2, the potential water savings originate from replacing the 5%−10% of fluid losses from the reservoir circulation rates into CO_2 sequestration. With mass flow rate on the order of 800 kg/s (10% loss) to 1600 kg/s (5%), the water savings from using $scCO_2$-EGS would be approximately 2 billion kg (0.5 billion gallons) of water each year, when compared to an equivalent water powered EGS system.

4.2. Emissions Savings. The proposed IGCC-EGS power plant has a cumulative net power output of 650 MWe. This would provide approximately 4.3 million MWh of energy each year. Replacing 15 billion kWh of conventional coal power with the clean power generation saves 78,000 tons of sulfur dioxide and 32,000 tons of nitrogen oxides emissions each year, and 1000 kg of CO_2 is saved for each MWh that is displaced by clean power.[29] Therefore, the combined IGCC-EGS plant will save emissions on the order of 8,200 tons of NO_x, 20,000 tons of SO_x, and 4.35 million tons of CO_2 emissions over one year when compared to a conventional fossil fuel power plant. The estimated net CO_2 avoided from power generation by the geothermal plant is 0.1 million tons of CO_2 per year. The remaining 4.25 million tons are the estimated CO_2 mitigated by sequestering the IGCC emissions in comparison to 550 MWe of conventional coal. Though conventional EGS has low emissions, the technology has a high water consumption rate. With IGCC, carbon capture and sequestration (CCS) systems typically increase the plants water consumption by 70%.[31] When these two systems are put together, the water consumption per unit of energy produced remains at the level of an IGCC plant without CCS, while reducing CO_2, NO_x, mercury, and SO_x emissions to new lows for coal based power technologies.

5. CONCLUSIONS

We explore the pairing of an integrated gasification combined cycle (IGCC) plant with an engineered geothermal system using supercritical CO_2 as the circulating fluid ($scCO_2$-EGS) and located in the environs of Albuquerque, NM. The IGCC plant generates electricity from the gasification of coal and the burning of the resulting hydrogen. Terminal effluents are water from the combustion of hydrogen and a pure stream of CO_2 that is consumed as makeup heat transfer fluid for the $scCO_2$-EGS. This pairing of IGCC-$scCO_2$-EGS reduces water usage, utilizes and partially sequesters byproduct $scCO_2$, and overall has reduced emissions and environmental impact in the closed-cycle system.

The site for this prototypical feasibility $scCO_2$-EGS project is located in the Rio Grande Rift Basin that stretches from south central Colorado into Mexico. The basin traverses a semiarid region of scarce water resources with a broadly distributed rural population that also concentrates into a few large population centers – most notably Albuquerque. The rift represents a region of higher than average heat flow with geothermal gradients reaching 39 °C/km and fractured crystalline basement rocks at depths of 2 to 7 km beneath the rift-filling sediments and older Mesozoic and Paleozoic formations.

The EGS reservoir will be developed in basement rocks at a depth of 5 km approximately 8 km to the southeast of Albuquerque. This location provides shallow access to the basement rocks as confirmed by the adjacent hydrocarbon exploration well, TransOcean Isleta 1, with an anticipated reservoir temperature of 200 °C. The EGS reservoir will be developed using a 5-spot pattern with an injector-producer separation of 500 m and with $scCO_2$ as the heat transfer fluid. For assumed fracture spacing of the order of 10 m and with single-well injection rates of 100 kg/s the time to 50% thermal drawdown in the reservoir is of the order of 30 years and triple that for more widely spaced (100 m) fractures. For an injection-recovery temperature differential of 60 °C−200 °C then a circulation rate of 100 kg/s of $scCO_2$ results in a thermal power output of 19 MW-thermal (per injector-withdrawal doublet of 100 kg/s). The $scCO_2$ production from the IGCC supplies the makeup fluid to compensate for leak-off losses in the EGS. For anticipated fluid losses of 5−10% the 80 kg/s output from the IGCC translates to 1600−800 kg/s overall flow rate distributed in 16−8 injectors each of ~100 kg/s, i.e. fugitive losses from the reservoir must be matched by the output from the IGCC. Thus the 80 kg/s is the 5% makeup amount corresponding to a constant circulation rate of 1600 kg/s. This translates to projected outputs from the EGS of the order of 150−300 MW-thermal that may decline to half of these values after 30 years. After the reservoir is depleted of heat, it may either be sealed and abandoned or drilled deeper or in different directions to access new reservoirs but to still take advantage of the existing surface plant and IGCC. The thermal recovery time is sufficiently long (centuries) that reuse is impractical unless the reservoir can be extended in its periphery, deepened, or used as a low enthalpy resource − the latter appearing impractical. Extending the reservoir at its periphery appears a desired trajectory as the boreholes to-depth may be retained in service, saving a significant additional capital cost to the extended-life project.

The generation of electrical power by integrated gasification combined cycle (IGCC) presents an environmentally closed system with high energy conversion efficiency. Specifically, fugitive gases of high purity, particularly CO_2, can be used for sequestration or in this case $scCO_2$-EGS. We design a plant with precombustion carbon capture as this allows the larger proportion of CO_2 to be captured as well as the capture of other pollutants. The principal components of a precombustion carbon-capture IGCC plant comprise processes of (i) oxygen production, (ii) oxy-gasification, (iii) the cleaning of the resulting synthesis-gas (iii) prior to burning and power generation and (iv) with the resulting pure stream of CO_2 used for $scCO_2$-EGS.

An order-of-magnitude economic analysis may be applied to the combined $scCO_2$-EGS-IGCC system. This determines the net present value (NPV) of the overall system and establishes probable payback periods based on the cost of electricity, possible electricity inflation rates, and the possibility of government funding for carbon capture and storage (CCS). The total capital cost and operational costs for the combined systems are $1.7 billion (IGCC) and $190 million (EGS), respectively. The assessment estimates that in the worst-case scenario (no increase in electricity prices and absent government funds to subsidize CCS) the system will pay for itself in its eighth year of operation. In this case the final present worth of the project over the 30 year lifetime would be $3 billion and have a return on investment (ROI) of 91%. The best-case scenario results in a payback time (PBT) of 6 years, a $5.5 billion total present worth over 30 years, and an ROI of 223%.

The prototypical project will minimize its impact on the local environment and residents through careful planning. The IGCC plant contains and processes the emissions that are commonly associated with coal-based power plants (CO_2, NOx, SOx, and water) with these much reduced and with the CO_2 actually turned into a resource as a heat transfer fluid. Potential impacts related to the EGS geothermal field are subsidence, groundwater contamination, and induced seismicity. At the planned 5 km depth of the EGS reservoir groundwater contamination is minimized if proper well construction procedures are followed. Due to the injection rates and close proximity of the proposed site to the city of Albuquerque induced seismicity may become an issue. This issue may only be addressed as the injection scheme is tuned, potentially involving reduced flow rates and alternating injectors and withdrawal wells as the response of the reservoir rocks is observed. The plant will save emissions of 8,200 tons of NOx, 20,000 tons of SO_2, and 4.35 million tons of CO_2 emissions each year to a comparable conventional coal power plant.

AUTHOR INFORMATION

Corresponding Author

*Phone: +1.814.865.2225. Fax: +1.814.865.3248. E-mail: elsworth@psu.edu.

Notes

Disclosure: This report was prepared as an account of work sponsored by an agency of the United States Government. Neither the United States Government nor any agency thereof, nor any of their employees, makes any warranty, express or implied, or assumes any legal liability or responsibility for the accuracy, completeness, or usefulness of any information, apparatus, product, or process disclosed, or represents that its use would not infringe privately owned rights. Reference herein to any specific commercial product, process, or service by trade name, trademark, manufacturer, or otherwise does not necessarily constitute or imply its endorsement, recommendation, or favoring by the United States Government or any agency thereof. The views and opinions of authors expressed herein do not necessarily state or reflect those of the United States Government or any agency thereof.

The authors declare no competing financial interest.

ACKNOWLEDGMENTS

This material is based upon work supported in part by the United States Department of Energy under Award Number DE-EE0002761 related to the 2011 National Student Geothermal Competition.

LIST OF ABBREVIATIONS

AGR = acid gas removal system
ASU = air separation unit
CCS = carbon capture and storage
DOE = Department of Energy
EGS = enhanced geothermal system
HRSG = heat recovery steam generator
HPST = high pressure steam turbine
IGCC = integrated gasification combined cycle
LCOE = levelized cost of electricity
NPV = net present value
PBT = payback time
PFM = parallel fracture model
ROI = return on investment
$scCO_2$-EGS = supercritical CO_2 in EGS
SRM = spherical reservoir model
WGS = water gas shift

REFERENCES

(1) Brown, D. In *Twenty-Fifth Workshop on Geothermal Reservoir Engineering*; Stanford University: 2000.
(2) Pruess, K. *Geothermics* **2006**, *35*, 351−367.
(3) Morgan, P.; Seager, W.; Golombek, M. *J. Geophys. Res.* **1986**, *91*, 6263−6276.
(4) Russell, L.; Snelson, S. *Memoirs-American Association of Petroleum Geologists* **1994**, 205−205.
(5) Kelley, V. *New Mexico Bureau of Mines & Mineral Resources* **1977**, 59.
(6) Grauch, V.; Hudson, M. *Geosphere* **2007**, *3.6*, 596−623.
(7) Blackwell, D.; Richards, M. *Geothermal Resources Council Transactions* **2004**, *28*, 317−320.
(8) Duffield, W.; Sass, J. *Geothermal energy: Clean power from the earth's heat*; DIANE, 2003; Vol. *1249*.
(9) Jiracek, G.; Swanberg, C.; Morgan, P.; Parker, M. *New Mexico Univ., Albuquerque (USA). Dept. of Geology, 1983*. 1983.
(10) Stone, W.; Mizell, N. *New Mexico Energy Institute* 1977.
(11) Johnson, R.; Finn, T.; Nuccio, V. *Potential for a Basin-centered Gas Accumulation in the Albuquerque Basin, New Mexico*; Johnson, R. C., Finn, T. M., Nuccio, V. F., Eds.; (2001). Potential for a Basin-centered Gas Accumulati US Department of the Interior, US Geological Survey, 2001.
(12) Elsworth, D. *J. Geophys. Res.* **1989**, *94*, 1927−1934.
(13) Lee, D.; Herman, J.; Elsworth, D. *KSCE J. Civil Eng.* **2011**, *15*, 679−687.
(14) Elsworth, D. *Geothermics* **1989**, *18*, 761−774.
(15) Gringarten, A.; Witherspoon, P. *Geothermics* **1973**, *2*, 119−122.
(16) Gringarten, A. *J. Geophys. Res.* **1975**, *80*, 1120.
(17) Elsworth, D. *J. Volcanol. Geotherm. Res.* **1990**, *44*, 283−293.

(18) Purcaru, G. *Tectonophysics* **1978**, *49*, 189−198.
(19) Taron, J.; Elsworth, D. *Int. J. Rock Mechanics Mining Sciences* **2010**, *47*, 1339−1348.
(20) Izadi, G.; Elsworth, D. *In 45th U.S. Rock Mechanics/Geomechanics Symposium* 2011.
(21) Mulyandasari, V.; Kolmetz, K. *KLM Technology Group* 2011.
(22) Wright, S.; Radel, R. *Sandia National Laboratories, Sandia Report SAND2010-0171*; 2010.
(23) Smith, A.; Klosek, J. *Fuel Process. Technol.* **2001**, *70*, 115−134.
(24) Platon, A.; Wang, Y. John Wiley & Sons: 2010; pp 311−328.
(25) Black, J. *National Energy Technology Laboratory* 2010, *1*.
(26) Chiesa, P.; Consonni, S. *J. Eng. Gas Turbines Power* **1999**, *121*, 295−305.
(27) Liu, K.; Song, C.; Subramani, V. *Hydrogen and syngas production and purification technologies;* 2010.
(28) Klara, J. *DOE/NETL-2007/1281*, 2007, *1*.
(29) Kagel, A.; Gawell, K. *The Electricity Journal* **2005**, *18*, 90−99.
(30) Matta, R.; Mercer, G.; Tuthill, R. *GE Power Systems* 2000.
(31) Shuster, E. *National Energy Technology Laboratory* 2008.

dx.doi.org/10.1021/ef301397n | *Energy Fuels* 2012, 26, 7378−7389